

1 Se isotopes as groundwater redox indicators:
2 Detecting natural attenuation of Se at an in situ
3 recovery U mine

4 *Anirban Basu^{1*#}, Kathrin Schilling^{2#}, Shaun T. Brown^{1,3}, Thomas M. Johnson⁴, John N.*
5 *Christensen³, Matt Hartmann⁵, Paul. W. Reimus⁶, Jeffrey M. Heikoop⁶, Giday Woldegabriel⁶,*
6 *Donald J. DePaolo^{1,3}*

7 ¹Department of Earth and Planetary Science, University of California, Berkeley, 307 McCone Hall,
8 Berkeley, CA, 94720, United States

9 ²Department of Environmental Science, Policy and Management, University of California, Berkeley, 130
10 Mulford Hall, Berkeley, CA, 94720, United States

11 ³Lawrence Berkeley National Laboratory, 1 Cyclotron Rd, Berkeley, CA, 94720, United States

12 ⁴Department of Geology, University of Illinois at Urbana-Champaign, 605 E. Springfield Avenue,
13 Champaign, Illinois, 61820, United States

14 ⁵Uranium Resources, Inc., 6950 S. Potomac St., Suite 300, Centennial, CO, 80112, United States

15 ⁶Earth and Environmental Sciences Division, Los Alamos National Laboratory, Los Alamos, NM, 87545,
16 United States

17 *Corresponding author: E-mail: anirbanbasu@berkeley.edu; phone: (510) 643 5062; fax: (510) 642
18 9520; #Authors contributed equally to this manuscript.

19 **ABSTRACT**

20 One of the major ecological concerns associated with in situ recovery (ISR) of uranium is the
21 environmental release of soluble, toxic Se-oxyanions generated by mining. Postmining natural
22 attenuation by the residual reductants in the ore body and reduced downgradient sediments
23 should mitigate the risk of Se contamination in groundwater. In this work, we investigate the Se
24 concentrations and Se isotope systematics of groundwater and of U ore bearing sediments from
25 an ISR site at Rosita, TX, USA. Our results show that selenate (Se(VI)) is the dominant Se
26 species in Rosita groundwater, and while several upgradient wells have elevated Se(VI), the
27 majority of the ore zone and downgradient wells have little or no Se-oxyanions. In addition, the
28 $\delta^{82}\text{Se}_{\text{VI}}$ of Rosita groundwater is generally elevated relative to the U ore up to +6.14‰, with the
29 most enriched values observed in the ore zone wells. Increasing $\delta^{82}\text{Se}$ with decreasing Se(VI)
30 conforms to a Rayleigh-type distillation model with an ϵ of $-2.25\text{‰} \pm 0.61\text{‰}$ suggesting natural
31 Se(VI) reduction occurring along the hydraulic gradient at the Rosita ISR site. Furthermore, our
32 results show that Se isotopes are excellent sensors for detecting and monitoring postmining
33 natural attenuation of Se oxyanions at ISR sites.

34 **Introduction**

35 The environmental mobility of the redox-active element Se is largely controlled by the high
36 solubility contrast between its oxidation states. The oxidized Se species (i.e., Se(VI) and Se(IV))
37 are highly soluble, mobile, and toxic at elevated concentrations. Se immobilization in the
38 environment occurs via chemical reduction to insoluble Se(0) or Se(-II). This redox-induced Se
39 immobilization is common during the formation of roll-front U ore deposits at redox interfaces in
40 groundwater systems. Information about key reactions involving Se in redox-interface mineral
41 deposits is crucial for understanding ore deposition mechanisms as well as pathways of Se
42 cycling in aqueous environments.

43 Reductive immobilization of Se is an important reaction that tends to concentrate Se in roll-
44 front type U ore deposits^{1,2}. Commonly, ferroselite (FeSe₂) and pyrite are host minerals for Se in
45 these U ore deposits¹⁻⁴. Compared to its average crustal concentration (0.05 mg/kg), high
46 concentrations of Se ranging from 0.5 - 500 mg/kg are reported from the roll-front deposits in
47 Wyoming, Montana, and Utah in the United States⁵⁻⁷. These anomalously high Se concentrations
48 have been used for uranium prospecting, particularly to characterize the location and shape of
49 roll-front type deposits⁸. The similarity between the redox potential for reduction of Se
50 oxyanions (Figure 1) and dissolved hexavalent uranium (U(VI))⁹⁻¹¹ leads to co-precipitation of
51 Se-minerals and U minerals.

52 In contrast, the oxidative dissolution of U ore enriched with Se minerals mobilizes Se and U in
53 the groundwater in their toxic, oxidized forms. Se in the effluent from a traditional U mining and
54 milling operation in northern Saskatchewan, Canada, led to accumulation of toxic levels of Se in
55 aquatic organisms^{12,13}. Elevated Se concentrations in runoff or aquifers are reported from the
56 regions of U mining and milling in the USA (e.g., Puerco River, Arizona; New Mexico; Rifle,

57 CO)^{14,15}. At present, almost all recent U mining in the USA and ~50% of global U mining
58 employs a mining technique known as in situ recovery (ISR) that extracts U by oxidative
59 dissolution of roll-front type sandstone-hosted ore deposits^{16,17}. Despite several advantages such
60 as the lack of mill tailings and radioactive dust, and its low CO₂ emission footprint, this mining
61 method releases Se as toxic, mobile Se oxyanions along with U(VI) directly into groundwater¹⁸.
62 Current strategies to mitigate Se(VI) in the groundwater after the completion of mining include
63 groundwater sweep and occasionally active remediation by biostimulation or injection of abiotic
64 reductants¹⁹.

65 Understanding naturally occurring reduction of Se-oxyanions is critical for designing efficient
66 remediation-restoration strategies at ISR sites. Natural attenuation of U(VI) by the existing
67 reducing environments downgradient of the redox interface at roll-front deposits has been
68 proposed as an inexpensive but effective remediation strategy. Recent work from our group
69 demonstrates conditions favorable for post-mining U(VI) reduction at ISR sites^{20,21}. After the
70 cessation of mining, the residual reducing capacity of the U ore and the prevailing reducing
71 environments downgradient of the ore should reduce mine-generated elevated concentrations of
72 toxic Se oxyanions. At pH 7, the redox potential (Eh) required for the reduction of Se oxyanions
73 (~0.4 V for Se(VI)/Se(IV) and ~0.2 V for Se(IV)/Se(0)) is higher than that for U(VI) (~0.0 V)⁹⁻
74 ¹¹, meaning that the reduction of Se(VI) and/or Se(IV) should precede U(VI) reduction. The
75 challenge is to identify the active reduction of Se in the ore zone and/or downgradient
76 groundwater and distinguish reduction from other processes that may affect aqueous Se
77 concentration such as sorption and dilution.

78 An effective approach to better understand important reactions and possibly the reactions
79 kinetics is the study of variations in stable isotope ratios. Se reduction can be detected by shifts

80 in the relative abundance of its stable isotopes (^{82}Se , ^{80}Se , ^{78}Se , ^{77}Se , ^{76}Se , ^{74}Se). The reduction of
81 Se(VI) to Se(0) or Se(-II) via the intermediate product Se(IV) induces a kinetic isotopic
82 fractionation resulting in the enrichment of heavier isotopes (i.e., ^{82}Se) in the remaining dissolved
83 Se oxyanions^{11, 22-24}. This enrichment is described in terms of an isotopic enrichment factor ϵ , a
84 per mil quantity, expressed as

$$85 \quad \epsilon = 1000\text{‰} * (\alpha - 1) \quad (1)$$

86 where α is the isotopic fractionation factor, defined as $\alpha = \frac{R_{product}}{R_{reactant}}$, where $R_{product}$ and
87 $R_{reactant}$ are the $^{82}\text{Se}/^{76}\text{Se}$ ratios in the reduction product and remaining Se oxyanions,
88 respectively. Relatively large isotopic fractionation factors are observed during microbial
89 reduction of Se(VI) to Se(IV) ($\epsilon \sim -8\text{‰}$) and of Se(IV) to elemental Se ($\epsilon \sim -14\text{‰}$)²⁵. Abiotic
90 reduction of Se(VI) by green rust or of Se(IV) by FeS also induces large fractionations (up to
91 -11‰)^{22,23,26}. In contrast, adsorption of Se(IV) to mineral surfaces results in a smaller
92 fractionation ($\sim -1\text{‰}$)^{26,27}. Thus, Se stable isotope ratios in groundwater are a more reliable
93 indicator of reduction of Se-oxyanions than aqueous concentrations of the Se species, which are
94 less easy to interpret because of the effects of dilution, removal by adsorption, or advection of
95 heterogeneous plumes past sampling points.

96 Although the release of potentially toxic Se oxyanions by ISR activity is a widespread
97 environmental risk, the fate of mobilized Se at postmining ISR sites is not yet well understood.
98 In this article, we present species-specific Se concentrations and isotopic measurement data for U
99 ore and 33 groundwater samples collected from wells located upgradient, within and
100 downgradient of a roll-front deposit located at an ISR site at Rosita, TX, USA. Sample locations
101 include both previously mined and unmined parts of the site. The objective of our study is to
102 demonstrate naturally occurring Se-oxyanion reduction at the site using Se isotope ratios of

103 groundwater samples collected across a groundwater redox interface. In addition, we discuss
104 how the Se isotope data may provide additional information about the redox condition in the
105 aquifer, particularly in the unmined part of the site, in relation to other geochemical indicators
106 (i.e., Se concentrations, U concentrations and U isotope data).

107 **Materials and Methods**

108 **Site description and Groundwater Sampling.** The study site is located at Rosita, TX, USA
109 (Figure 2). A detailed description of the site can be found in Basu et al., 2015²⁰. Briefly, the U
110 roll-front deposit at this ISR site is defined by a poorly consolidated, mineralized sand unit
111 bounded above and below by low permeability clay units. For ISR mining, site groundwater
112 fortified with O₂ and H₂O₂ was injected into the ore zone in 3 mining units or production area
113 authorizations (PAA) to oxidize and dissolve the U ore utilizing the high natural bicarbonate
114 concentrations to stabilize U-CO₃ complexes. The mining unit PAA 4 has a complete set of
115 monitoring wells but no mining has occurred to date. The mining was followed by a restoration
116 process, except in the most recently mined PAA 3, where the site groundwater treated by reverse
117 osmosis was injected back into the aquifer. A network of existing wells, drilled within,
118 upgradient and downgradient of the ore body, was used for postmining monitoring of the site.
119 The baseline (BL) wells located within the production zone was used for monitoring the water
120 quality in the ore zone while the upgradient and downgradient monitoring wells (MW) were used
121 to ensure that there was no excursion of the mining or restoration fluid leaving the ore zone.

122 Groundwater samples were collected from 33 wells along transects roughly parallel to the
123 current groundwater flow direction. The wells were purged prior to sampling, and samples for
124 Se-oxyanion concentrations and Se isotopes were filtered using 0.45 µm in-line filters and

125 collected in pre-cleaned HDPE bottles with no headspace and no preservatives. The samples
126 were stored at 4 °C prior to analysis.

127 **Sediment digestion.** U ore samples were obtained from a borehole adjacent to BL 39 in PAA
128 4 (Figure 2). For Se concentration and isotopic analysis, 1.0 g aliquots of sediment samples from
129 7 discrete depths were digested in an acid mixture (concentrated HCl + concentrated HNO₃, 3:1
130 v/v). First, each 1.0 g aliquot was treated with 4 mL of ~7 M HNO₃ in Teflon beakers at 80 °C
131 for about 12 hrs to remove any carbonate from the sediments. The remaining HNO₃ was then
132 evaporated to near dryness at 60 °C prior to addition of a freshly prepared acid mixture of HCl
133 and HNO₃. The samples were digested at 80 °C for 24 hr. After digestion, the acid mixture was
134 removed by evaporating to near dryness at 70 °C, and 5 mL of 0.1 N HCl was added. This
135 solution was filtered using 0.45 µm PTFE filters to remove undigested particles.

136 **Sample Purification and Mass Spectrometry.** Se isotope ratios were measured using multi-
137 collector inductively coupled plasma mass spectrometry (MC- ICP-MS) at the Department of
138 Geology, University of Illinois, Urbana-Champaign following the methods described in Schilling
139 et al., 2014, 2015^{28,29}. For isotopic measurements, we used a double spike technique (⁷⁴Se + ⁷⁷Se)
140 to correct for the isotopic fractionation during mass spectrometry, and any that might occur
141 during sample purification by ion-exchange chromatography^{28,29}. An aliquot of the double spike
142 solution of appropriate species (either Se(IV) or Se(VI)) was added to a carefully weighed
143 aliquot of the sample (groundwater, or digested U ore) containing approximately 100 ng of Se.

144 The Se-oxyanion species was purified from other Se species and matrix elements by ion
145 exchange chromatography²⁹. For the separation of Se(VI), the samples were first acidified with
146 HCl to a final strength not exceeding 0.1 M HCl. The acidified samples were passed through the
147 anion exchange resin (Eichrom Technologies, LLC) where Se(VI) was adsorbed onto the resin

148 while Se(IV) and other matrix elements (e.g., As, Ge) were rinsed out by 0.1 M HCl. Se(VI) was
149 eluted from the resin by 6M HCl and heated to 105 °C for 1 hr. Finally, the samples were diluted
150 to 2 M HCl, sparged with N₂ to remove a volatile Br species, and equilibrated with Kr in the air
151 for 12 hr prior to isotopic analysis.

152 For Se(IV) extraction, the samples were not acidified before loading on the anion exchange
153 resin. The Se(VI) was adsorbed onto the resin and the effluent containing Se(IV) was collected
154 by rinsing with 0.1 M HCl, then oxidized to Se(VI) by treatment with K₂S₂O₈ at 100 °C for 1 hr.
155 After oxidation, all samples were purified using the above procedure for Se(VI) purification.

156 For purification of Se from the digested U ore (as Se(IV)), we first evaporated the samples to
157 near dryness and then re-dissolved them in 5 mL 0.1 M HCl. An aliquot of this solution
158 containing ~ 100 ng Se was brought to a strength of 4-6 M HCl prior to purification by hydride
159 generation described in ref 30. The H₂Se was trapped in a mixture of NaOH and H₂O₂ and
160 converted to Se(VI). The excess H₂O₂ was removed from the samples by heating (~ 100 °C) prior
161 to purification using the procedure for Se(VI) described above.

162 Se isotope ratios are reported as δ⁸²Se relative to the isotopic standard reference material NIST
163 SRM 3149³¹, defined as

$$164 \quad \delta^{82}\text{Se} = \left[\frac{(^{82}\text{Se}/^{76}\text{Se})_{\text{sample}}}{(^{82}\text{Se}/^{76}\text{Se})_{\text{SRM3149}}} - 1 \right] \times 1000\text{‰} \quad (2)$$

165 The uncertainty (2σ) of δ⁸²Se measurements, calculated from the twice the root mean square
166 (RMS, 95% confidence level)³² of 24 duplicate sample preparations and analysis, was 0.17‰.

167 The value of the isotopic fractionation factor (α) was determined from the slope of the best-fit
168 line from the linearized plot of ln(δ⁸²Se + 1000‰) vs. ln(Se(VI))³³. The uncertainties (2σ) of ε
169 were ± 0.6‰, calculated from the scatter of the data points around the best-fit line using standard
170 linear estimation methods.

171 **Results and Discussion**

172 **Se Concentrations in Rosita Groundwater and U Ore.** We have quantified Se(VI) and
173 Se(IV) concentrations in the Rosita groundwater (Table 1) to understand the distribution pattern
174 of the aqueous Se species at the study site. Se(VI) is the dominant species with concentrations up
175 to 306 µg/L in the groundwater samples while Se(IV) is found in fewer samples and only at
176 concentrations below 9 µg/L. Generally, except for ore zone wells BL 3 and BL 4, groundwater
177 from the upgradient monitoring wells has higher Se(VI) compared to that in the ore zone or
178 downgradient monitoring wells. We did not observe any systematic pattern in the distribution of
179 Se(IV) at the site. Out of 12 samples with measurable Se(IV), 3 ore zone wells (BL 7, BL 29 and
180 BL 34) and one downgradient well, MW 37, contain only Se(IV) while the rest contain both
181 Se(VI) and Se(IV). In the previously mined parts of the site, the downgradient monitoring wells
182 MW 37, MW 75, MW 85, and MW 89, contain little (<1 µg/L) or no Se-oxyanions, either as
183 Se(VI) or Se(IV). The wells MW 32, MW 102, MW 103 and MW 137, located directly
184 downgradient of the mapped discontinuities of the ore body (Figure 2), contain substantial
185 amount of Se(VI) and in some cases Se(IV). In the unmined PAA 4, the downgradient wells
186 show little dissolved Se: MW 149 has no Se-oxyanions whereas MW 144 contains 0.6 µg/L
187 Se(VI) and Se(IV) below detection level (<0.1 µg/L).

188 The Se concentrations in the U ore collected at 7 discrete depths from borehole OZCH3
189 adjacent to the ore zone well BL 39 in the unmined PAA4 area, are low and vary from 24 µg/kg
190 to 48 µg/kg (Table 1). There is no apparent trend in the Se concentrations with depth. However,
191 the samples with the highest U concentrations collected from 70.71 – 71.32 m below the ground
192 surface also contain the highest amount of Se. The U ore was not characterized for the identity of

193 Se bearing minerals, but previous work identified ferroselite and elemental Se as the dominant
194 Se bearing species in South Texas and other roll-front type U deposits^{1,2,34-37}.

195 **Se Isotope Ratios in Rosita Groundwater and U Ore.** The $\delta^{82}\text{Se}$ in groundwater samples from
196 all PAAs and in the U ore are provided in Table 1. The $\delta^{82}\text{Se}$ of aqueous Se(VI) varies from
197 -1.46‰ to $+6.14\text{‰}$, with most of the samples showing elevated $\delta^{82}\text{Se}$ relative to the Se isotope
198 standard SRM 3149 (i.e., $\delta^{82}\text{Se} > 0.0\text{‰}$) (Figure 3). The highest $\delta^{82}\text{Se}$ of Se(VI) is observed in
199 groundwater from the ore zone well BL 39 from the unmined PAA4 area, while BL 3 from the
200 already mined PAA1 exhibits the most depleted $\delta^{82}\text{Se}$ value (-1.46‰). In a subset of samples
201 there is an apparent trend of increasing $\delta^{82}\text{Se}_{\text{VI}}$ with decreasing Se(VI) (Figure 3). Contrary to the
202 $\delta^{82}\text{Se}$ values of Se(VI), $\delta^{82}\text{Se}$ of Se(IV) is substantially depleted by up to -6.45‰ , except in
203 samples from BL 29 ($\delta^{82}\text{Se}_{\text{IV}} = 0.51\text{‰}$) and BL 34 ($\delta^{82}\text{Se}_{\text{IV}} = 0.73\text{‰}$). Notably, these wells had
204 no measurable Se(VI). In the samples containing both Se oxyanion species, Se(IV) is isotopically
205 lighter than Se(VI) with $\Delta^{82}\text{Se}$ ($\approx \delta^{82}\text{Se}_{\text{VI}} - \delta^{82}\text{Se}_{\text{IV}}$) ranging from 3.5‰ to 6.9‰ . We observe a
206 weak correlation between Se(IV) concentration and $\delta^{82}\text{Se}_{\text{IV}}$ of the groundwater samples; the
207 $\delta^{82}\text{Se}_{\text{IV}}$ decreases with decreasing Se(IV) (Figure S1).

208 The Se isotope compositions of the Se minerals in the U ore from 7 discrete depths are
209 provided in Table 1. The $\delta^{82}\text{Se}$ of the U ore ranges from -1.28‰ to -0.40‰ . The median value
210 of -0.72‰ is low relative to the majority of the groundwater Se(VI) samples (Figure 3). There is
211 also an enrichment in $\delta^{82}\text{Se}$ in the ore with increasing depth.

212 **Implication of Se Isotopic Signature of Rosita U ore.** Our observations of ^{82}Se depletion of
213 the ore are limited to a single borehole (OZCH3) in PAA4, which does not provide the full extent
214 of the spatial variability in $\delta^{82}\text{Se}$ of the ore body. Furthermore, the U ore samples from the
215 borehole OZCH3 are not representative of the Se-enriched portion of the roll-front system

216 generated by reductive precipitation of Se. Lower Se concentrations of the U ore compared to
217 that of upgradient groundwater suggest a Se rich sediment upgradient of the borehole OZCH3
218 (Table 1, Figure 3). This is further supported by our observation of ^{82}Se depletion in the U ore.
219 Ideally, reductive precipitation of Se-oxyanions at the redox interface should produce ^{82}Se
220 depleted Se minerals at the upgradient fringe of the roll-front deposit. With increasing distance
221 along the hydraulic gradient, the Se minerals should become isotopically heavier. However, after
222 complete removal of Se-oxyanions from the groundwater, the Se concentrations and isotopic
223 composition of the sediments should return to background values. The sediments collected 6m
224 above the ore-bearing zone contain 24.3 $\mu\text{g}/\text{kg}$ of Se with a $\delta^{82}\text{Se}$ of -1.54‰ , resembling the ore-
225 zone sediments both in terms of Se concentrations and isotopic composition (Table 1).
226 Therefore, we surmise that Se concentrations and isotopic compositions of our U ore samples
227 reflect the primary Se content of the aquifer sediments.

228 **Se Reduction in Groundwater: Se Concentration Distribution and Geochemical**
229 **Conditions.** The distribution of dissolved Se in Rosita groundwater is consistent with reduction
230 of Se oxyanions, particularly Se(VI) reduction, by naturally occurring reducing environments
231 within and downgradient of the ore zone. The Se(VI) hotspots at the upgradient wells or ore zone
232 wells in the mined part of the site resulted from the oxidation of Se minerals either during mining
233 or by interaction with the oxygenated recharge water. For example, high Se(VI) up to 107 $\mu\text{g}/\text{L}$
234 in the upgradient wells MW 158 and MW 154 in the unmined PAA 4 is likely to reflect natural
235 dissolution of Se minerals in the aquifer. In absence of any Se removal within or downgradient
236 of the ore zone, the downgradient wells should show Se(VI) concentrations similar to that of the
237 upgradient wells. Little or no Se oxyanions in the downgradient wells, particularly in MW 37,
238 MW 75, MW 85, and MW 89, suggests Se removal before groundwater arrives at these wells.

239 The observed removal of Se along the hydraulic gradient is consistent with the geochemical
240 conditions conducive to reduction of Se-oxyanions within and downgradient of the ore zone. At
241 the study site, a progression from nitrate-reducing, to Fe(III)-reducing, and then to U(VI)-
242 reducing conditions along the hydraulic gradient is inferred from concentrations of the redox
243 species (e.g., NO_3^- , Fe(II) and U(VI)), Eh values and isotopic measurements (e.g., $\delta^{15}\text{N}$, and
244 $\delta^{238}\text{U}$) of groundwater samples²⁰. Briefly, a general decrease in NO_3^- concentrations along the
245 hydraulic gradient and a linear relation between the $\delta^{18}\text{O}$ -nitrate and $\delta^{15}\text{N}$ -nitrate ($r^2 =$
246 0.77 , $n = 11$) with a slope ($\Delta\delta^{18}\text{O}/\Delta\delta^{15}\text{N}$) of 0.73 ± 0.13 is indicative of microbial
247 denitrification. In addition, localized zones of Fe(III) and Mn(IV) reduction is suggested
248 by elevated dissolved Mn (>0.05 mg/ L) and Fe (>0.1 mg/L) concentrations in
249 groundwater samples from PAA1, PAA2, and PAA3. Furthermore, decreasing Eh of
250 samples downgradient of the ore zone (except MW 32, MW 102, MW 103, MW 137) in
251 all previously mined PAAs also consistent with the pattern observed for redox sensitive
252 aqueous species. Among the downgradient wells investigated by Basu et al. (2015), the samples
253 from MW 37, MW 75, MW 85, and MW 89 exhibited low Eh (-11.7 mV to -105.5 mV), low
254 U(VI) concentrations (< 20 $\mu\text{g/L}$) and highly depleted $\delta^{238}\text{U}$ (-1.41‰ to -2.49‰) suggesting
255 naturally occurring reducing environments capable of U(VI) and thus, Se(VI) reduction.

256 The overall range of Eh and pH suggests thermodynamic favorability of Se-oxyanions
257 reduction in Rosita groundwater (Figure 1). The decrease in Se(VI) along the hydraulic gradient
258 is therefore consistent with the Se(VI) and perhaps Se(IV) reduction in downgradient the
259 reducing environments suggested by Basu et al. 2015 based on U isotopes and other evidence.
260 Alternatively, Se(IV) could be strongly adsorbing and removed via sorption onto minerals.

261 Several downgradient wells, however, do not follow the general trend of aqueous Se(VI)
262 removal along the hydraulic gradient. These wells, MW 32, MW 102, MW 103, and MW 137,
263 are located directly downgradient of the mapped gaps in the ore body (Figure 2). These gaps may
264 mark regions that lacked the reducing materials that were responsible for the formation of the ore
265 body in the adjacent areas. This difference implies an unrestricted flow of the upgradient water
266 rich in Se(VI) and other oxidants (e.g., NO_3^-) (Figure S2) and with a high Eh to the downgradient
267 wells MW 32, MW 102, MW 103, and MW 137 through these gaps, which is consistent with the
268 observations reported in reference 20. The postmining restoration fluid with high residual Se(VI)
269 is unlikely to arrive at the downgradient wells due to low groundwater velocity (3-6 m/year) and
270 restriction of flow by net withdrawal of groundwater during restoration. However, the presence
271 of the reduction product Se(IV) in MW 32 and MW 103 suggest existing Se(VI) reducing
272 conditions in these wells which is also supported by our Se isotope data (see below).

273 **Se Reduction in Groundwater: Se Isotope Ratios.** If all of the variation of $\delta^{82}\text{Se}$ were due to
274 reduction of Se from a single Se source by a single mechanism, a strong correlation between
275 $\delta^{82}\text{Se}$ and concentrations of Se-oxyanions would be expected. We did not observe a strong
276 correlation between $\delta^{82}\text{Se}$ and Se(VI) concentrations which suggests heterogeneous Se sources
277 and complex Se cycling mechanisms. However, the samples that exhibit highly enriched $\delta^{82}\text{Se}$
278 (e.g., $\delta^{82}\text{Se} > 4\text{‰}$) can only be generated by reduction of Se(VI). In the following paragraphs, we
279 discuss the evidence of Se(VI) reduction from the $\delta^{82}\text{Se}$ data from Rosita groundwater along
280 with potential alternative mechanisms with their limitations.

281 In addition to the distribution of Se-oxyanion concentrations, Se isotope data from Rosita U
282 ore and groundwater samples help identify pathways of Se-cycling and delineate Se(VI) reducing
283 zones at the study site. The upgradient groundwater currently entering the roll-front system is

284 Se(VI)-rich with concentrations ranging from 32 $\mu\text{g/L}$ to 137 $\mu\text{g/L}$ (median Se(VI) = 94.84
285 $\mu\text{g/L}$). The $\delta^{82}\text{Se}$ of the upgradient groundwater also varies from -1.12‰ to $+2.22\text{‰}$, with an
286 average $\delta^{82}\text{Se}$ of 0.51‰ . Since the roll-front system reduces and captures all incoming Se(VI),
287 we hypothesize that the average $\delta^{82}\text{Se}$ of the U ore should be identical to the average $\delta^{82}\text{Se}$ of
288 incoming groundwater, assuming that the Se inputs for the U ore were similar to that observed in
289 the present system.

290 If dissolution of Se minerals were the only mechanism responsible for the observed
291 distribution of Se(VI) in Rosita groundwater, we would expect the groundwater samples to be
292 similar to the inferred average $\delta^{82}\text{Se}$ of the U ore ($\sim 0.5\text{‰}$). The oxidative dissolution of U ore
293 should yield aqueous Se(VI) with similar isotopic composition as quantitative layer-by-layer
294 dissolution of Se mineral grains results in negligible isotopic fractionation. However, it is
295 possible for the postmining groundwater to acquire Se with a range of $\delta^{82}\text{Se}$ values (e.g., -1.5‰
296 to $\sim 2\text{‰}$), because we expect the isotopic composition of Se minerals to exhibit spatial variability
297 in the ore zone. Aqueous Se isotope compositions outside the -1.5‰ to $+2.0\text{‰}$ range suggest an
298 alternate or additional process affecting the Se isotope composition of the groundwater.

299 The enrichments in $\delta^{82}\text{Se}$ of Rosita groundwater relative to the inferred average $\delta^{82}\text{Se}$ of the U
300 ore are likely caused by Se(VI) reduction in Rosita groundwater. With ongoing reduction of
301 Se(VI), the unreacted remaining Se(VI) exhibits ^{82}Se enrichment^{11, 22-27,30}, while the intermediate
302 product Se(IV) is first enriched in the lighter isotopes (i.e., ^{76}Se), and later upon further reduction
303 to Se(0) and possibly complete removal of Se(VI), is enriched in ^{82}Se . The largest $^{82}\text{Se}_{\text{VI}}$
304 enrichments observed in the ore zone wells BL 17 and BL 39 are 5.19‰ and 6.14‰ ,
305 respectively, suggesting a maximum offset of $\sim 6\text{‰}$ from that of the inferred $\delta^{82}\text{Se}$ of the U ore.
306 In all samples containing both Se(VI) and Se(IV), Se(IV) is isotopically lighter (i.e. enriched in

307 ^{76}Se , $-6.38\text{‰} < \delta^{82}\text{Se} < 0\text{‰}$). This suggests that Se(IV) is a product of Se(VI) reduction rather than
308 arising from the oxidation of the U ore. In addition, the two groundwater samples with $^{82}\text{Se}_{\text{IV}}$
309 enrichment (i.e., $\delta^{82}\text{Se}_{\text{IV}} > 0\text{‰}$) have low Eh ($\text{Eh}_{\text{BL } 29} = -82.5 \text{ mV}$ and $\text{Eh}_{\text{BL } 34} = -59.4 \text{ mV}$) and
310 no detectable Se(VI). This ^{82}Se enrichment in Se(IV) and a lack of Se(VI) suggests extensive
311 reduction of Se(IV) has occurred in the absence of production of Se(IV) via Se(VI) reduction.

312 The correlation between Se isotopic shifts and changes in Se oxyanion concentrations also
313 suggests aqueous Se(VI) reduction. When Se(VI) data from all wells are pooled together, we
314 observe two distinct trends in the relationship between $\delta^{82}\text{Se}$ values and Se(VI) concentrations
315 (Figure 2). First, there is an increasing trend in $\delta^{82}\text{Se}$ with decreasing Se(VI). Second, for several
316 wells such as BL 8, BL 10, MW 102, MW 103, MW 53, and MW 137, Se(VI) concentrations
317 decrease with no major shift in the $\delta^{82}\text{Se}$. In samples showing no major change in $\delta^{82}\text{Se}$,
318 particularly in BL 8, BL 10, MW 102, and MW 103, the decrease in Se(VI) may be attributed to
319 a localized mixing with groundwater with relatively low Se, similar to that of MW 42, which is
320 also consistent with relatively high Eh values and NO_3^- concentrations (Figure S2) in these
321 wells²⁰. Alternatively, a more likely scenario is that these samples may have acquired variable
322 amounts of Se from the Se-rich zone in the roll-front with a $\delta^{82}\text{Se}$ similar to the inferred average
323 $\delta^{82}\text{Se}$ of the roll-front. The first trend where $\delta^{82}\text{Se}$ in a subset of samples increased with
324 decreasing Se(VI) conforms to a Rayleigh-type fractionation model with $\epsilon = -2.25\text{‰} \pm 0.61\text{‰}$
325 calculated excluding Se data from the wells containing measurable NO_3^- . This strongly suggest
326 Se(VI) reduction as the primary mechanism of Se(VI) concentration decrease in these samples.

327 Two alternative mechanisms, mixing and equilibrium isotopic exchange, with the potential to
328 influence the Se isotopic signature of Rosita groundwater are unlikely to play any major role at
329 the study site. The elevation in $\delta^{82}\text{Se}$ of Se(VI) in BL 39 and BL 17 above $\sim 2\text{‰}$ cannot be

330 generated by mixing ore-zone groundwater with an average $\delta^{82}\text{Se}$ of 0.5‰ with the upgradient
331 water entering the system with a maximum $\delta^{82}\text{Se}$ of ~2‰. Therefore, mixing cannot account for
332 the observed elevated $\delta^{82}\text{Se}$ values of Se(VI) in BL 39 and BL 17. Also, an equilibrium isotopic
333 exchange between coexisting dissolved species Se(VI) and Se(IV) or more reduced Se species
334 would lead to ^{82}Se enrichment in Se(VI). This seems highly unlikely under the prevalent
335 geochemical conditions that are far from chemical equilibrium. The rates of exchange between
336 Se(VI) and Se(IV), which requires transfer of two electrons, have yet to be determined.
337 However, based on recent reports on U(VI)-U(IV) exchange also requiring two electrons
338 transferred³⁸, very slow exchange (100 to 1000 yrs) between Se(VI) and Se(IV) may be inferred
339 at very low concentrations (i.e. < 9 $\mu\text{g/L}$) of Se(IV). In addition, Se(VI)-Se(IV) exchange may
340 further be inhibited by removal of Se(IV) by either adsorption or by reduction to Se(0)^{11,39}.

341 **Se Isotopes as Redox Indicators in the Unmined Area.** In addition to serving as an indicator
342 for reduction of potentially toxic Se-oxyanions in groundwater, the results from the unmined
343 PAA 4 area demonstrate that stable Se isotope ratios aid in the precise determination of the redox
344 state of the aquifer at Rosita ISR site (Table S1). Our previous work on U isotope ratios
345 ($^{238}\text{U}/^{235}\text{U}$, expressed as $\delta^{238}\text{U}$)²⁰ showed evidence of U(VI) reduction in the transect containing
346 MW 158, BL 36, and MW 144 along the hydraulic gradient, particularly in the ore zone BL and
347 the downgradient well, while there was a lack of U(VI) reducing conditions along another
348 transect (MW 154, BL 39, MW 149) (Figure 2, Table S1). Along both transects, a decrease in
349 NO_3^- in groundwater from ≥ 12 mg/L in the upgradient wells to below detection in the ore zone
350 BL wells and downgradient wells was also reported²⁰. The western transect, where the lack of a
351 large ^{238}U depletion in groundwater indicated the absence of U(VI) reduction in the ore zone well
352 BL 39 ($\delta^{238}\text{U} = 0.56\text{‰}$) and downgradient MW 149 ($\delta^{238}\text{U} = 0.48\text{‰}$), shows an overall

353 enrichment in $\delta^{82}\text{Se}$ of Se(VI) up to $\sim 6\%$ relative to the average $\delta^{82}\text{Se}$ (0.5%) of the U ore with
354 BL 39 exhibiting a $\delta^{82}\text{Se}$ of 6.14% . This $\delta^{82}\text{Se}$ of Se(VI) in BL 39 is $\sim 4\%$ higher compared to
355 that of the upgradient well MW 154 ($\delta^{82}\text{Se} = 2.19\%$). Se(VI) in the downgradient well MW 149
356 is below the detection limit ($< 0.1 \mu\text{g/L}$). This suggests progressively stronger Se(VI) reducing
357 conditions along the hydraulic gradient.

358 In comparison, the upgradient well MW 158 ($\delta^{238}\text{U} = -0.08\%$) from the western transect
359 shows ^{82}Se depletion ($\delta^{82}\text{Se}_{\text{VI}} = -1.12\%$) with a lower Se(VI) concentration suggesting spatial
360 heterogeneity both in terms of background Se content and isotopic composition. However, the
361 wells along the hydraulic gradient in this transect with highly fractionated U isotope ratios, BL
362 36 ($\delta^{238}\text{U} = -1.61\%$) and MW 144 ($\delta^{238}\text{U} = -1.96\%$) have very little or no detectable Se
363 oxyanions suggesting either almost quantitative reduction of Se(VI) and Se(IV) and/or removal
364 of Se(IV) via adsorption onto aquifer material. Thus the results from the unmined PAA4
365 demonstrate the effectiveness of Se isotope ratios in delineating Se(VI) reducing environments
366 and in providing additional information about existing redox conditions that can not be obtained
367 from the U isotopic data alone.

368 **Fractionation Mechanisms at Rosita and Comparison of ϵ with Previous Studies.** The
369 magnitude of the Se isotope fractionation observed at Rosita is more consistent with a microbial
370 reduction mechanism than with abiotic reduction, but there is still sufficient uncertainty that
371 abiotic reduction cannot be ruled out. Johnson et al. 2011 provides a detailed review of the
372 magnitudes of Se isotope fractionation for various abiotic reductants and microbial species.
373 Microbial reduction of Se-oxyanions yields a range of ϵ values, spanning from -0.3% to -7.5%
374 for the reduction of Se(VI) to Se(IV) and from -1.7% to -12% for the reduction of Se(IV) to
375 Se(0). The abiotic reduction of Se generally yields consistently large ($> -10\%$) isotopic

376 fractionations. The ϵ for reduction of Se(VI) to Se(IV) by the Fe(II)-Fe(III) layered double
377 hydroxide mineral “green rust”, a likely reductant in soils and sediments, is $\sim -11\%$ while the
378 reduction to Se(IV) to Se(0) by FeS and NH_2OH or ascorbic acid produces a fractionation (as ϵ)
379 of -10% , and -15.0 to -19.2% , respectively. The ϵ determined from the groundwater samples
380 from the Rosita ISR site ($-2.25\% \pm 0.61\%$) is much small compared to that observed during
381 abiotic Se(VI) reduction and falls within the range observed during Se(VI) reduction by natural
382 microbial consortia²⁴. Despite some heterogeneities, the observed sequence of redox reactions
383 along the hydraulic gradient from NO_3^- reducing to Fe(III)- and U(VI)-reducing environments is
384 also consistent with the microbially mediated redox ladder in aquifers⁴⁰. However, reservoir
385 effects arising from the lack of chemical communication between the zones of reduction (e.g.,
386 biofilms, or mineral surfaces in clay-rich zones) and the bulk dissolved Se(VI) in the more
387 rapidly flowing parts of the sandy aquifer may limit the expression of overall isotopic
388 fractionation in groundwater samples and thus lead to a diminished apparent ϵ value³⁰. Future
389 research involving similar sites should be directed toward identification of the Se reduction
390 mechanism and determination of ϵ at the site using analysis of the temporal trend of Se-oxyanion
391 concentrations with Se isotope ratios from the target wells. Additionally, the ϵ determined from
392 the field data should be complemented by laboratory experiments for the site-specific reduction
393 mechanism.

394 **Implications for Monitoring of Se and U Reduction at ISR sites.** The results of this study
395 demonstrate that Se isotope ratios are effective indicators of natural attenuation of Se(VI), a
396 residual product of ISR mining and a potential water contaminant for several ISR sites.
397 Furthermore, our results suggest that the Se isotope ratios record the redox environments

398 precursory to U(VI) reducing conditions that cannot be obtained from the concentration (e.g.,
399 Se(VI) or U(VI)) data alone.

400 A groundwater monitoring approach combining Se isotope ratios with U isotopic
401 measurements is therefore advantageous in determining conditions conducive for postmining
402 natural attenuation of contaminants at ISR sites. For instance, naturally occurring aqueous and
403 adsorbed Fe(II)^{41,42}, magnetite^{43,44} and titanomagnetite⁴⁵, and FeS^{46,47} (both residual after mining
404 and biogenic) may readily reduce U(VI) in aquifers. These abiotic reductants are also capable of
405 reducing Se(IV)⁴⁸⁻⁵¹. Thus, in addition to $\delta^{238}\text{U}$, $\delta^{82}\text{Se}$ of groundwater would provide an improved
406 characterization of the existing redox state and reducing capacity of the aquifer. In aquifers with
407 a need for active remediation, the knowledge of the existing redox state is also important to
408 determine the remediation strategy and the choice of reductant (if used) to avoid aggressive
409 reductive remediation, which may mobilize contaminants such as arsenic.

410 Our measurements on Se speciation and stable Se isotopes reveal the spatial distribution at a
411 single time and do not provide direct information on time-dependent changes in Se oxyanion
412 concentrations and concomitant changes in Se isotope ratios. Efficient post-mining monitoring of
413 reduction would include time series measurements of Se oxyanion concentration and Se isotope
414 ratios in samples from the target ore zone BL wells or wells from the monitoring ring. This
415 would enable more accurate determination of the exact relationship between the changes in
416 Se(VI) and/or Se(IV) concentrations in a target well and the associated shifts in $\delta^{82}\text{Se}$ (or the
417 site-specific isotopic fractionation factor), which is required for the quantification of Se(VI)
418 remediation.

419 **Acknowledgements.** This research was funded by the UC Laboratory Fees Research Program.
420 We thank Uranium Resources, Inc. for providing site access and logistic support during sample

421 collection and drilling. The US Dept of Energy provided salary support for DJD and JNC during
422 the study period under Contract No. DE-AC02-05CH11231. We thank two anonymous
423 reviewers and Associate Editor Daniel Giammar for constructive comments that improved the
424 quality of this manuscript.

425 **Associated Content.** Correlation between $\delta^{82}\text{Se}_{\text{IV}}$ and Se(IV), and distribution of NO_3^- in
426 Rosita groundwater Comparison between Se(VI) and U(VI) concentrations in groundwater from
427 PAA 4 along with Se ($\delta^{82}\text{Se}$) and U isotope ratios ($\delta^{238}\text{U}$), are provided in the Supporting
428 Information. This information is available free of charge via the Internet at <http://pubs.acs.org>.

429 **References**

- 430 (1) Howard, J. H. Geochemistry of selenium: formation of ferroselite and selenium behavior
431 in the vicinity of oxidizing sulfide and uranium deposits. *Geochim. Cosmochim. Acta*
432 **1977**, *41* (11), 1665–1678.
- 433 (2) Dahlkamp, F. J. *Uranium deposits of the world*; Springer, Germany, 2009.
- 434 (3) Granger, H. C.; Warren, C. G. Unstable sulfur compounds and the origin of roll-type
435 uranium deposits. *Econ. Geol.* **1969**, *64* (2), 160–171.
- 436 (4) Xiong, Y. Predicted equilibrium constants for solid and aqueous selenium species to 300
437 °C: applications to selenium-rich mineral deposits. *Ore Geol. Rev.* **2003**, *23* (3-4), 259–
438 276.
- 439 (5) Beath, O. A.; Hagner, A. F.; Gilbert, C. S. *Some rocks and soils of high selenium*
440 *content*; Vol. 36, University of Wyoming, 1946.
- 441 (6) Dribus, J. R.; Nanna, R. F. *National uranium resource evaluation, Rawlins quadrangle,*
442 *Wyoming and Colorado*; Bendix Field Engineering Corp., Grand Junction, CO (USA),
443 1982.
- 444 (7) Plant, J. A.; Bone, J.; Voulvoulis, N.; Kinniburgh, D. G.; Smedley, P. L.; Fordyce, F.
445 M.; Klinck, B. Arsenic and selenium. In *Treaties on Geochemistry (Second Edition)*;
446 Holland, H. D., Turekian, K. K., Eds.; Elsevier, Oxford, 2014; pp 13-57.
447 [doi:10.1016/B978-0-08-095975-7.00902-5](https://doi.org/10.1016/B978-0-08-095975-7.00902-5).
- 448 (8) Bartz, G. L. Uranium prospecting based on selenium and molybdenum. US Patent
449 Document 4,345,912/A/; U.S. Commissioner of Patents, Washington, DC. 1982.
- 450 (9) Maher, K.; Bargar, J. R.; Brown, G. E., Jr. Environmental Speciation of Actinides.
451 *Inorg. Chem.* **2013**, *52* (7), 3510–3532.
- 452 (10) Seby, F.; Potin-Gautier, M.; Giffaut, E.; Borge, G. A critical review of thermodynamic
453 data for selenium species at 25 C. *Chem. Geol.* **2001**, *171* (3-4), 173–194.
- 454 (11) Johnson, T. M. Stable Isotopes of Cr and Se as Tracers of Redox Processes in Earth
455 Surface Environments. In *Handbook of environmental isotope geochemistry*; Baskaran,
456 M., Ed.; Springer, Berlin, Heidelberg, 2011; pp 155–175.
- 457 (12) Muscatello, J. R.; Belknap, A. M.; Janz, D. M. Accumulation of selenium in aquatic
458 systems downstream of a uranium mining operation in northern Saskatchewan, Canada.
459 *Environ. Pollut.* **2008**, *156* (2), 387–393.
- 460 (13) Muscatello, J. R.; Bennett, P. M.; Himbeault, K. T.; Belknap, A. M.; Janz, D. M. Larval
461 Deformities Associated with Selenium Accumulation in Northern Pike (*Esox lucius*)
462 Exposed to Metal Mining Effluent. *Environ. Sci. Technol.* **2006**, *40* (20), 6506–6512.
- 463 (14) Van Metre, P. C.; Gray, J. R. Effects of uranium mining discharges on water quality in
464 the Puerco River basin, Arizona and New Mexico. *Hydrolog. Sci. J.* **1992**, *37* (5), 463–
465 480.
- 466 (15) Williams, K. H.; Wilkins, M. J.; N'Guessan, A. L.; Arey, B.; Dodova, E.; Dohnalkova,
467 A.; Holmes, D.; Lovley, D. R.; Long, P. E. Field evidence of selenium bioreduction in a
468 uranium-contaminated aquifer. *Environ. Microbiol. Rep.* **2013**, *5* (3), 444–452.
- 469 (16) *Uranium 2011: Resources, Production and Demand*. A joint report by the OECD
470 Nuclear Energy Agency and the International Atomic Energy Agency: Paris, France,
471 2012; <http://www.oecd-nea.org/ndd/pubs/2012/7059-uranium-2011.pdf>.
- 472 (17) *Uranium 2014: Resources, Production and Demand*. A joint report by the OECD
473 Nuclear Energy Agency and the International Atomic Energy Agency: Paris, France,

- 474 2014; <https://www.oecd-nea.org/ndd/pubs/2014/7209-uranium-2014.pdf>.
- 475 (18) Ramirez, P., Jr; Rogers, B. P. Selenium in a Wyoming Grassland Community Receiving
476 Wastewater from an In Situ Uranium Mine. *Arch. Environ. Contam. Toxicol.* **2002**, *42*
477 (4), 431–436.
- 478 (19) Davis, J. A.; Curtis, G. P. *Consideration of geochemical issues in groundwater*
479 *restoration at uranium in-situ leach mining facilities (NUREG/CR-6870)*; Division of
480 Fuel, Engineering, and Radiological Research, Office of Nuclear Regulatory Research,
481 US Nuclear Regulatory Commission; Washington, DC, 2007.
- 482 (20) Basu, A.; Brown, S. T.; Christensen, J. N.; DePaolo, D. J.; Reimus, P. W.; Heikoop, J.
483 M.; Woldegabriel, G.; Simmons, A. M.; House, B. M.; Hartmann, M. Isotopic and
484 Geochemical Tracers for U(VI) Reduction and U Mobility at an in Situ Recovery U
485 Mine. *Environ. Sci. Technol.* **2015**, *49* (10), 5939–5947.
- 486 (21) Brown, S. T.; Basu, A.; Christensen, J. N.; Reimus, P. W.; Heikoop, J. M.; Simmons, A.
487 M.; WoldeGabriel, G.; Maher, K.; Weaver, K.; Clay, J. Isotopic evidence for reductive
488 immobilization of uranium across a roll-front mineral deposit. *Environ. Sci. Technol.*
489 **2016**, doi.10.1021/acs.est.6b00626.
- 490 (22) Johnson, T. M.; Bullen, T. D. Mass-Dependent Fractionation of Selenium and
491 Chromium Isotopes in Low-Temperature Environments. *Rev. Mineral. Geochem.* **2004**,
492 *55* (1), 289–317.
- 493 (23) Johnson, T. M.; Bullen, T. D. Selenium isotope fractionation during reduction by Fe (II)-
494 Fe (III) hydroxide-sulfate (green rust). *Geochim. Cosmochim. Acta* **2003**, *67* (3), 413–
495 419.
- 496 (24) Ellis, A. S.; Johnson, T. M.; Herbel, M. J.; Bullen, T. D. Stable isotope fractionation of
497 selenium by natural microbial consortia. *Chem. Geol.* **2003**, *195* (1-4), 119–129.
- 498 (25) Herbel, M. J.; Johnson, T. M.; Oremland, R. S.; Bullen, T. D. Fractionation of selenium
499 isotopes during bacterial respiratory reduction of selenium oxyanions. *Geochim.*
500 *Cosmochim. Acta* **2000**, *64* (21), 3701–3709.
- 501 (26) Mitchell, K.; Couture, R.-M.; Johnson, T. M.; Mason, P. R. D.; Van Cappellen, P.
502 Selenium sorption and isotope fractionation: Iron(III) oxides versus iron(II) sulfides.
503 *Chem. Geol.* **2013**, *342* (C), 21–28.
- 504 (27) Johnson, T. M.; Herbel, M. J.; Bullen, T. D.; Zawislanski, P. T. Selenium isotope ratios
505 as indicators of selenium sources and oxyanion reduction. *Geochim. Cosmochim. Acta*
506 **1999**, *63* (18), 2775–2783.
- 507 (28) Schilling, K.; Johnson, T. M.; Mason, P. R. D. A sequential extraction technique for
508 mass-balanced stable selenium isotope analysis of soil samples. *Chem. Geol.* **2014**, *381*
509 (C), 125–130.
- 510 (29) Schilling, K.; Johnson, T. M.; Dhillon, K. S.; Mason, P. R. D. Fate of selenium in soils
511 at a seleniferous site recorded by high precision Se isotope measurements. *Environ. Sci.*
512 *Technol.* **2015**, *49* (16), 9690–9698.
- 513 (30) Clark, S. K.; Johnson, T. M. Effective Isotopic Fractionation Factors for Solute Removal
514 by Reactive Sediments: A Laboratory Microcosm and Slurry Study. *Environ. Sci.*
515 *Technol.* **2008**, *42* (21), 7850–7855.
- 516 (31) Carignan, J.; Wen, H. Scaling NIST SRM 3149 for Se isotope analysis and isotopic
517 variations of natural samples. *Chem. Geol.* **2007**, *242* (3-4), 347–350.
- 518 (32) Hyslop, N. P.; White, W. H. Estimating Precision Using Duplicate Measurements. *J. Air*
519 *Waste Manage. Assoc.* **2009**, *59* (9), 1032–1039.

- 520 (33) Scott, K. M.; Lu, X.; Cavanaugh, C. M.; Liu, J. S. Optimal methods for estimating
521 kinetic isotope effects from different forms of the Rayleigh distillation equation.
522 *Geochim. Cosmochim. Acta* **2004**, 68 (3), 433–442.
- 523 (34) Reynolds, R. L.; Goldhaber, M. B. Iron disulfide minerals and the genesis of roll-type
524 uranium deposits. *Econ. Geol.* **1983**, 78 (1), 105–120.
- 525 (35) Reynolds, R. L.; Goldhaber, M. B. Origin of a South Texas Roll-Type Uranium Deposit
526 .1. Alteration of Iron-Titanium Oxide Minerals. *Econ. Geol.* **1978**, 73 (8), 1677–1689.
- 527 (36) Huang, W. H. Geochemical and sedimentologic problems of uranium deposits of Texas
528 Gulf Coastal Plain. *AAPG Bulletin* **1978**, 62, 1049–1062.
- 529 (37) Granger, H. C. Ferroselite in a roll-type uranium deposit, Powder River Basin,
530 Wyoming. *US Geological Survey Professional Paper* **1966**, C133–C137.
- 531 (38) Wang, X.; Johnson, T. M.; Lundstrom, C. C. Low temperature equilibrium isotope
532 fractionation and isotope exchange kinetics between U(IV) and U(VI). *Geochim.*
533 *Cosmochim. Acta* **2015**, 158, 1–14.
- 534 (39) White, A. F.; Benson, S. M.; Yee, A. W.; Wollenberg, H. A.; Flexser, S. Groundwater
535 contamination at the Kesterson Reservoir, California: 2. Geochemical parameters
536 influencing selenium mobility. *Water Resour. Res.* **1991**, 27 (6), 1085–1098.
- 537 (40) McMahon, P. B.; Chapelle, F. H. Redox Processes and Water Quality of Selected
538 Principal Aquifer Systems. *Ground Water* **2008**, 46 (2), 259–271.
- 539 (41) Du, X.; Boonchayaanant, B.; Wu, W.-M.; Fendorf, S.; Bargar, J.; Criddle, C. S.
540 Reduction of Uranium(VI) by Soluble Iron(II) Conforms with Thermodynamic
541 Predictions. *Environ. Sci. Technol.* **2011**, 45 (11), 4718–4725.
- 542 (42) Taylor, S. D.; Marcano, M. C.; Rosso, K. M.; Becker, U. An experimental and ab initio
543 study on the abiotic reduction of uranyl by ferrous iron. *Geochim. Cosmochim. Acta*
544 **2015**, 156, 154–172.
- 545 (43) Latta, D. E.; Gorski, C. A.; Boyanov, M. I.; O’Loughlin, E. J.; Kemner, K. M.; Scherer,
546 M. M. Influence of Magnetite Stoichiometry on U^{VI} Reduction. *Environ. Sci. Technol.*
547 **2012**, 46 (2), 778–786.
- 548 (44) Yuan, K.; Renock, D.; Ewing, R. C.; Becker, U. Uranium reduction on magnetite:
549 Probing for pentavalent uranium using electrochemical methods. *Geochim. Cosmochim.*
550 *Acta* **2015**, 156, 194–206.
- 551 (45) Latta, D. E.; Pearce, C. I.; Rosso, K. M.; Kemner, K. M.; Boyanov, M. I. Reaction of U^{VI}
552 with Titanium-Substituted Magnetite: Influence of Ti on U^{IV} Speciation. *Environ. Sci.*
553 *Technol.* **2013**, 47 (9), 4121–4130.
- 554 (46) Veeramani, H.; Scheinost, A. C.; Monsegue, N.; Qafoku, N. P.; Kukkadapu, R.;
555 Newville, M.; Lanzirotti, A.; Pruden, A.; Murayama, M.; Hochella, M. F., Jr. Abiotic
556 Reductive Immobilization of U(VI) by Biogenic Mackinawite. *Environ. Sci. Technol.*
557 **2013**, 47 (5), 2361–2369.
- 558 (47) Troyer, L. D.; Tang, Y.; Borch, T. Simultaneous Reduction of Arsenic(V) and
559 Uranium(VI) by Mackinawite: Role of Uranyl Arsenate Precipitate Formation. *Environ.*
560 *Sci. Technol.* **2014**, 48 (24), 14326–14334.
- 561 (48) Myneni, S.; Tokunaga, T. K.; Brown, G. E. Abiotic selenium redox transformations in
562 the presence of Fe(II,III) oxides. *Science* **1997**, 278 (5340), 1106–1109.
- 563 (49) Scheinost, A. C.; Charlet, L. Selenite Reduction by Mackinawite, Magnetite and
564 Siderite: XAS Characterization of Nanosized Redox Products. *Environ. Sci. Technol.*
565 **2008**, 42 (6), 1984–1989.

- 566 (50) Charlet, L.; Scheinost, A. C.; Tournassat, C.; Greneche, J. M.; Géhin, A.; Fernández-
567 Martí'nez, A.; Coudert, S.; Tisserand, D.; Brendle, J. Electron transfer at the
568 mineral/water interface: Selenium reduction by ferrous iron sorbed on clay. *Geochim.*
569 *Cosmochim. Acta* **2007**, *71* (23), 5731–5749.
- 570 (51) Baik, M. H.; Lee, S. Y.; Jeong, J. Sorption and reduction of selenite on chlorite surfaces
571 in the presence of Fe(II) ions. *J. Environ. Radioact.* **2013**, *126*, 209–215.

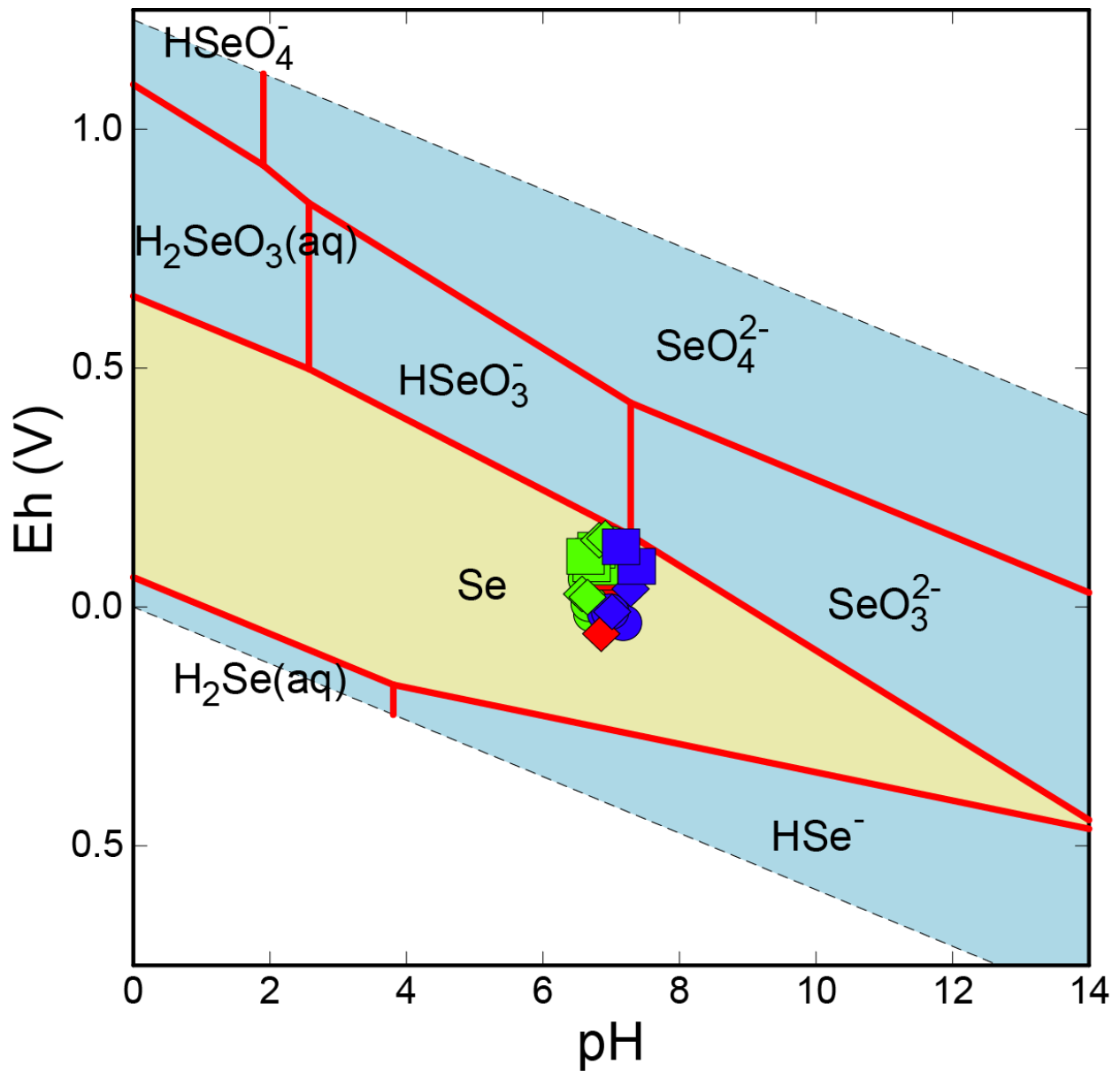
572 Table 1. Se concentrations and isotope ratios in Rosita groundwater and U ore (ND = Not
 573 determined). Eh measurements are from Basu et al., 2015.

Rosita Groundwater							
Well	Location	PAA	Se(VI) µg/L	δ⁸²Se_{VI}	Se(IV) µg/L	δ⁸²Se_{IV}	Eh (mV)
BL 3	Ore zone	1	306.06	-1.46‰	<0.1		
BL 4	Ore zone	1	44.02	0.97‰	<0.1		-6.0
BL 7	Ore zone	1	<0.1		8.78	-1.36‰	-37.5
BL 8	Ore zone	1	6.08	0.82‰	<0.1		46.4
BL 9	Ore zone	2	<0.1		<0.1		9.2
BL 10	Ore zone	2	9.32	0.97‰	<0.1		81.2
BL 17	Ore zone	2	12.51	5.19‰	<0.1		-64.5
BL 22	Ore zone	2	<0.1		<0.1		-42.6
BL 28	Ore zone	3	<0.1		<0.1		-62.7
BL 29	Ore zone	3	<0.1		3.18	0.51‰	-82.5
BL 34	Ore zone	3	<0.1		8.22	0.73‰	-59.4
MW 25	Upgradient	1	59.87	0.58‰	8.17	-2.92‰	23.3
MW 26	Upgradient	1	112.27	0.9‰	0.4	ND	56.5
MW 32	Downgradient	1	66.56	0.45‰	1.29	-6.45‰	56.1
MW 37	Downgradient	1	<0.1		0.15	-2.63‰	-105.5
MW 42	Upgradient	2	<0.1		<0.1		34.0
MW 45	Upgradient	2	106.62	-0.47‰	0.61	ND	69.5
MW 53	Upgradient	2	31.59	0.83‰	0.24	ND	40.5
MW 66	Upgradient	2	63.87	0.7‰	<0.1		56.5
MW 75	Downgradient	3	<0.1		<0.1		-11.7
MW 85	Downgradient	2	<0.1		<0.1		-22.3
MW 89	Downgradient	2	<0.1		<0.1		-29.0

MW 102	Downgradient	2	10.38	1.12‰	<0.1		90.2
MW 103	Downgradient	2	6.26	0.59‰	0.2	-4.66‰	94.2
MW 129	Upgradient	3	137.01	0.43‰	4.35	-3.69‰	35.4
MW 131	Upgradient	3	94.84	0.54‰	<0.1		76.5
MW 137	Downgradient	3	29.72	0.51‰	<0.1		-59.5
BL 36	Ore zone	4	<0.1		<0.1		
BL 39	Ore zone	4	8.97	6.14‰	2.87	-0.61‰	
MW144	Downgradient	4	0.6	ND	<0.1		
MW149	Downgradient	4	<0.1		<0.1		
MW154	Upgradient	4	107.44	2.22‰	<0.1		
MW158	Upgradient	4	48.83	-1.12‰	<0.1		

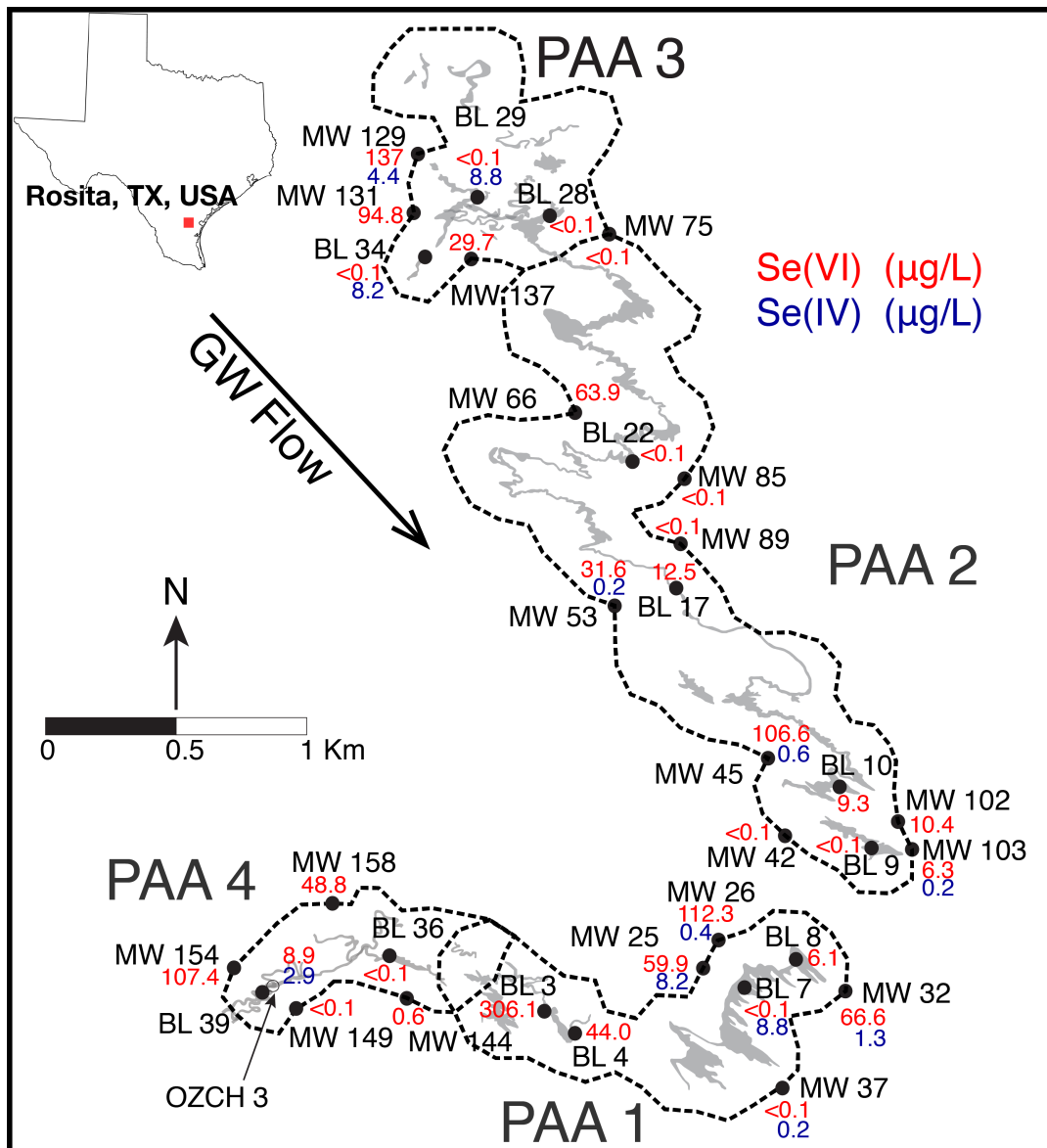
Rosita U ore

Depth b.g.s (m)	Se (µg/kg)	$\delta^{82}\text{Se}$
60.66 - 60.96 (background)	24.3	-1.54‰
66.14 - 66.45	36.8	-1.28‰
66.45 - 66.75	33.8	-0.85‰
66.75 - 67.06	30.8	-0.62‰
67.06 - 67.21	31.7	-0.79‰
70.71 - 71.02	47.6	-0.64‰
71.02 - 71.32	39.0	-0.40‰

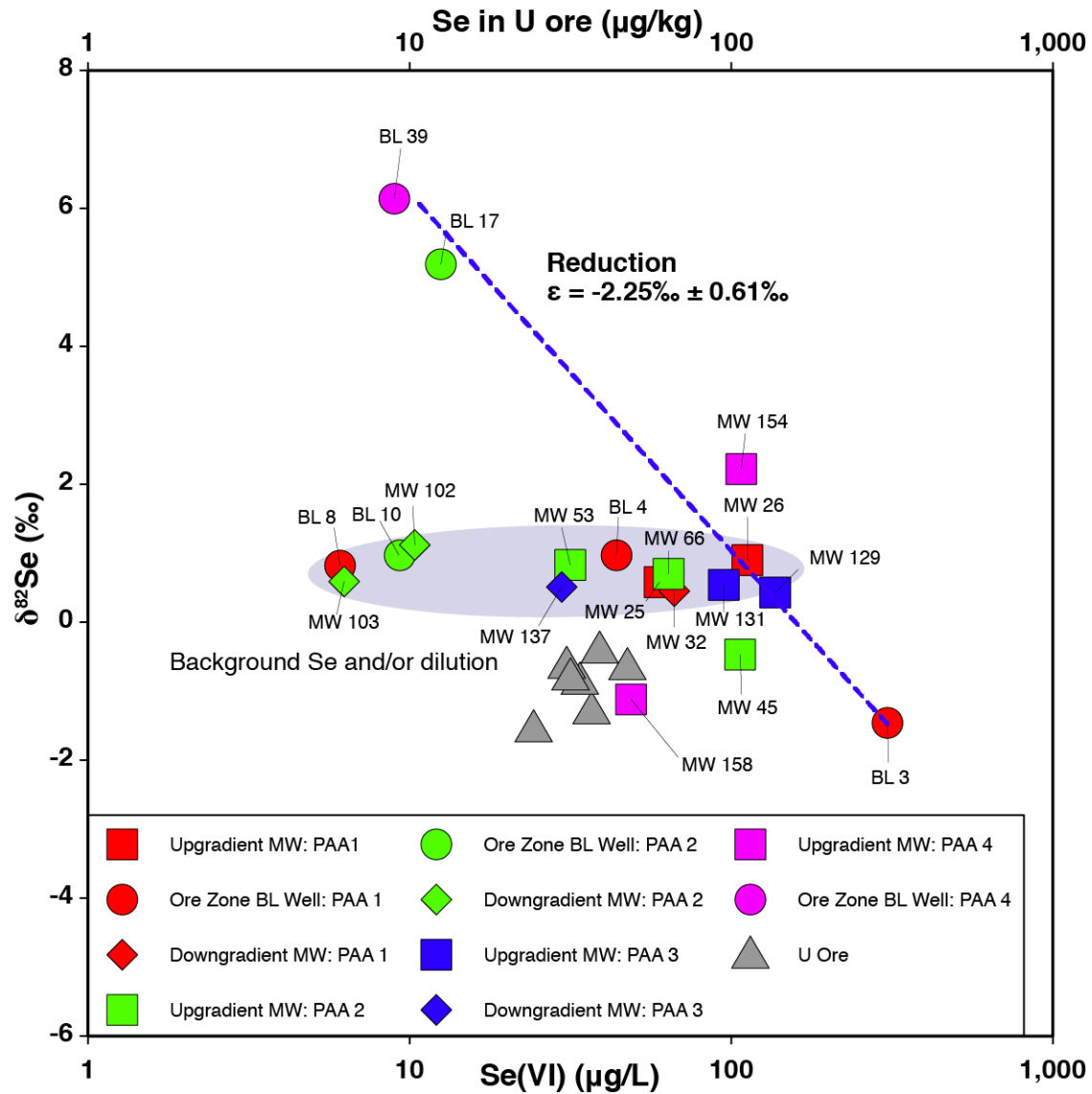


575

576 Figure 1. Pourbaix diagram for Se showing the thermodynamic stability of different Se species in
 577 the environment. Total Se concentration is 10^{-6} M. Light blue fields represent aqueous species,
 578 golden field represents solid Se species. Red, green, and blue symbols represent groundwater
 579 from mining units PAA 1, PAA 2, and PAA 3, respectively. Squares, circles and diamonds
 580 represent groundwater samples from upgradient, ore zone and downgradient wells, respectively.

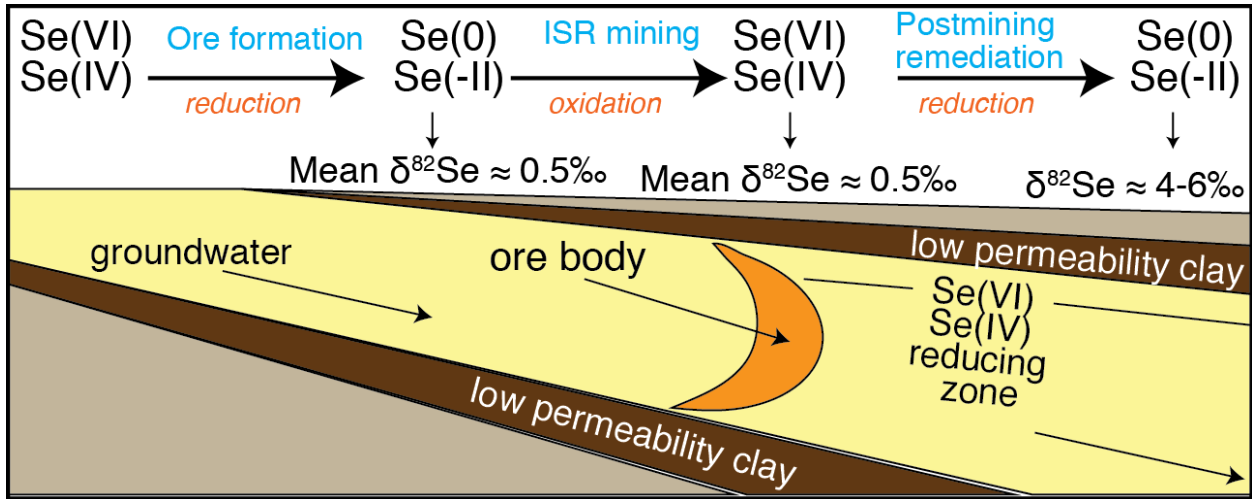


581 Figure 2. Map of the Rosita ISR site showing the mining units (PAA) and the distribution of
 582 Se(VI). Light gray areas define the roll-front U deposit. Black dots represent locations of wells
 583 sampled for Se oxyanion and Se isotope measurements and the open circle shows the location of
 584 the borehole for the U ore sample. The dotted lines represent the perimeter ring of the monitoring
 585 wells. Numbers represent Se-oxyanion concentrations - Se(VI) (red) and Se(IV) (blue) in µg/L.
 586



587

588 Figure 3. $\delta^{82}\text{Se}$ of aqueous Se(VI) in Rosita groundwater and Se minerals in the U ore vs. Se
 589 concentration. Gray triangles represent the U ore and red, green blue and pink symbols represent
 590 groundwater from mining units PAA 1, PAA 2, PAA 3, and PAA 4, respectively. The error bars
 591 ($2 \times \text{s.e.}$) for are smaller than the size of the symbols. The blue dotted line represent the modeled
 592 $\delta^{82}\text{Se}$ using a Rayleigh distillation model with $\epsilon = -2.25\text{‰} \pm 0.61\text{‰}$ excluding the samples with
 593 NO_3^- .



594

595 TOC art.

596